Synthesis, Structure, and Electrochemistry of an Electron Deficient μ-Oxo Porphyrin Dimer, $[(TPPBr_4)Fe]_2O$

Karl M. Kadish,*,† Marie Autret,† Zhongping Ou,† Pietro Tagliatesta,*,‡ Tristano Boschi,‡ and Vincenzo Fares*,§

Department of Chemistry, University of Houston, Houston, Texas 77204-5641, Dipartimento di Scienze e Tecnologie Chimiche, Università degli Studi di Roma, Tor Vergata, 00133 Roma, Italy, and Istituto di Chimica dei Materiali, Area delle Ricerca di Roma/Montelibretti, via Salaria Km 29.300-C.P.10, 00016 Monterotondo, Roma, Italy

Received January 12, 1996[⊗]

The synthesis and structural and electrochemical properties of an electron deficient iron μ-oxo porphyrin dimer, (μ-oxo)bis[(2,3,12,13-tetrabromo-5,10,15,20- tetraphenylporphyrinatoiron(III)), represented as $[(TPPBr_4)Fe]_2O$, are reported. X-ray analysis indicates an Fe−O−Fe angle of 177.9(5)° and an interplanar distance of 4.58 Å between the two mean porphyrin planes. Opposite pyrrole rings on the same macrocycle are twisted by about 25° relative to each other so that the porphyrin skeleton distortion is best described as a twisted saddle-shaped configuration. Electrochemical studies reveal that the highly halogenated μ-oxo dimer is stable in PhCN and *undergoes four one-electron oxidations and four one-electron reductions in a total of seven steps.* The singly reduced and singly oxidized forms of the dimer were characterized by thin-layer spectroelectrochemistry and ESR spectroscopy.

The use of electron deficient metalloporphyrins as catalysts for reactions with molecular oxygen has led to the synthesis and characterization of various highly halogenated porphyrins.[1] Of special interest is the electrochemistry of this type of compound since the half-wave potentials for oxidation or reduction may be related either directly or indirectly to the catalytic efficiency for oxidation of hydrocarbons.[1,2] The redox potentials might also be used to determine the degree of macrocycle distortion since distorted monomeric porphyrins containing bulky or electron-withdrawing substituents may be easier to oxidize than related planar porphyrins not containing these groups.[3−6] In addition, distorted monomeric porphyrins often exhibit reductions which follow linear free energy relations involving the number of added substituents but oxidations which do not in that they are much more facile than expected on the basis of purely inductive effects.[3−6]

In this regard, it should be noted that the available electrochemical data on porphyrins containing a high degree of substitution at the β-pyrrole positions of the macrocycle has been obtained almost exclusively for monomeric complexes due, in large part, to the fact that porphyrin dimers having sterically hindered macrocycles are not readily formed. We have now obtained one such μ-oxo dimer and, in the present paper, report its electrochemical, spectral, and structural properties. The investigated compound is (μ-oxo)bis[(2,3,12,13-tetrabromo-5,-10,15, 20-tetraphenylporphyrinato)iron(III)], which is represented as $[(TPPBr_4)Fe]_2O$.[7,9]

Crystals of $[(TPPBr_4)Fe]_2O{\cdot}2EtOH{\cdot}H_2O$ suitable for X-ray analysis were obtained by slow diffusion of *n*-hexane into a chloroform/1% ethanol solution containing the μ-oxo iron

† University of Houston.
‡ Università degli Studi di Roma.
§ Istituto di Chimica dei Materiali.
⊗ Abstract published in *Advance ACS Abstracts,* December 15, 1996.

(1) (a) *The Activation of Dioxygen and Homogeneous Catalytic Oxidation*; Barton, D. H. R., Martell, A. E., Sawyer, D. T., Eds.; Plenum Press: New York, 1993. (b) *Metalloporphyrins in Catalytic Oxidations*; Shelton, R. A., Ed.; Marcel Dekker, Inc.: New York, 1994.
(2) (a) Ellis, P. E., Jr. *Catal. Lett.* **1989**, *3*, 389. (b) Lyons, J. E.; Ellis, P. R., Jr. *Catal. Lett.* **1991**, *8*, 45. (c) Ellis, P. E., Jr.; Lyons, J. E. *Coord. Chem. Rev.* **1990**, *105*, 181. (d) Ellis, P. E., Jr.; Lyons, J. E. *J. Chem. Soc., Chem. Commun.* **1989**, 1189. (e) Ellis, P. E., Jr.; Lyons, J. E. *J. Chem. Soc., Chem Commun.* **1989**, 1315.
(3) (a) Kadish, K. M.; D'Souza, F.; Villard, A.; Autret, M.; Van Caemelbecke, E.; Bianco, P.; Antonini, A.; Tagliatesta, P. *Inorg. Chem.* **1994**, *33*, 5169. (b) Tagliatesta, P.; Li, J.; Autret, M.; Van Caemelbecke, E.; Villard, A.; D'Souza, F.; Kadish, K. M. *Inorg. Chem.* **1996**, *35*, 5570.
(4) (a) D'Souza, F.; Villard, A.; Van Caemelbecke, E.; Franzen, M.; Boschi, T.; Tagliatesta, P.; Kadish, K. M. *Inorg. Chem.* **1993**, *32*, 4042.
(5) (a) Reddy, D.; Ravikanth, M.; Chandrashekar, T. K. *J. Chem. Soc., Dalton Trans*. **1993**, 3575. (b) Barkigia, K. M.; Berber, M. D.; Fajer, J.; Medforth, C. J.; Renner, M.; Smith, K. M. *J. Am. Chem. Soc.* **1990**, *112*, 8851. (c) Shelnutt, J. A.; Medforth, C. J.; Berber, M. D.; Barkigia, K. M.; Smith, K. M. *J. Am. Chem. Soc*. **1991**, *113*, 4077. (d) Sparks, L. D.; Medforth, C. J.; Park, M. S.; Chamberlain, J. R.; Ondrias, M. R.; Senge, M. O.; Smith, K. M.; Shelnutt, J. A. *J. Am. Chem. Soc.* **1993**, *115*, 581.
(6) (a) Hodge, J. A.; Hill, M. G.; Gray, H. B. *Inorg. Chem.* **1995**, *34*, 809. (b) Giraudeau, A.; Ezahr, I.; Gross, M.; Callot, H. J.; Jordan, J. *Bioelectrochem. Bioenerg.* **1976**, *3*, 519. (c) Wijesekera, T.; Matsumoto, A.; Dolphin, D.; Lexa, D. *Angew. Chem., Int. Ed. Engl*. **1990**, *29*, 1028. (d) Richter, S. A.; Tsang, P. K. S.; Sawyer, D. T. *Inorg. Chem.* **1989**, *28*, 2471. (e) Ochsenbein, P.; Ayougou, K.; Mandon, D.; Fisher, J.; Weiss, R.; Austin, R. N.; Jayaraj, K.; Gold, A.; Terner, J.; Fajer, J. *Angew. Chem., Int. Ed. Engl*. **1994**, *33*, 348. (f) Giraudeau, A.; Callot, H. J.; Gross, M. *Inorg. Chem*. **1979**, *18*, 201.
(7) Synthesis of $[(TPPBr_4)Fe]_2O$. Method A: $(TPPBr_4)H_2$[6a] (300 mg) was dissolved in a solution of dry toluene (50 mL) degassed under argon. $Fe(CO)_5$ (20 mL) and then 20 mg of iodine were added to the solution, which was kept at 60 °C for 5 h under argon and then 12 h under air at room temperature. The solvent was evaporated and the residue purified on silica gel (elution: $CHCl_3$/*n*-hexane, 1:1). The first eluted fraction was evaporated and the residue recrystallized from $CHCl_3$/*n*-hexane to give $[(TPPBr_4)Fe]_2O$ in a yield of 80%. Method B: $(TPPBr_4)FeCl$[6b] (200 mg) was dissolved in 50 mL of THF, after which 20 mL of a 20% KOH solution was added. The mixture was stirred at room temperature for 12 h and, after addition of $CHCl_3$ (120 mL), was washed twice with 100 mL of water. The solution was dried over Na_2SO_4, the solvent was evaporated under vacuum, and the residue was purified as described in the first procedure. $[(TPPBr_4)Fe]_2O$ was obtained in a 45% yield.
(8) (a) Callot, H. J. *Bull. Soc. Chim. Fr*. **1974**, *7, 8*, 1492. (b) Groves, J. T.; Myers, R. S. *J. Am. Chem. Soc*. **1983**, *105*, 5791.
(9) $[(TPPBr_4)Fe]_2O$ MS (FAB/NBA): *m*/*z* 1984 (100) $[M + H]^+$. UV−vis (PhCN): λ_{max} (nm) ($\epsilon \times 10^{-4}$ mol^{-1} L cm^{-1}) 419 (14.5), 598 (2.3), 631 (2.2). Elemental analysis calculated for $[(TPPBr_4)Fe]_2O$: C, 53.68; H, 2.28; N, 5.58. Found: C, 53.47; H, 2.44; N, 5.65.

S0020-1669(96)00040-7 CCC: $14.00

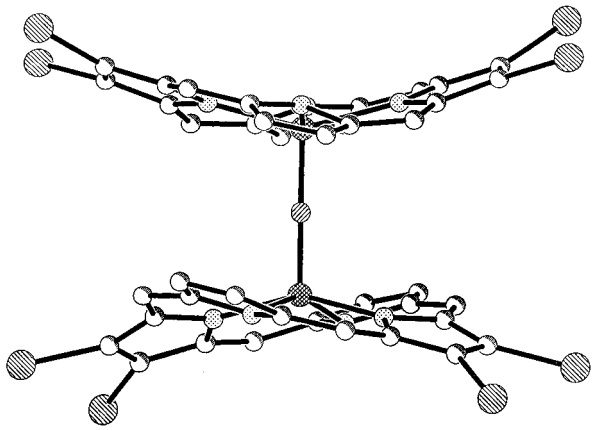

Figure 1. Side view of $[(TPPBr_4)Fe]_2O$ (phenyl rings have been omitted for clarity). The atoms have been represented as spheres for clarity.

complex.[10] The molecular structure of $[(TPPBr_4)Fe]_2O$ is shown in Figure 1. The unit cell contains four, nearly iso-oriented, $[(TPPBr_4)Fe]_2O$ μ-oxo dimers. Large holes between the dimers accommodate water and highly disordered alcohol molecules.

The Fe−O−Fe angle is 177.9(5)°, and there is an interplanar distance of 4.58 Å between the two porphyrin 24-atom core mean planes. The two Fe−O distances in $[(TPPBr_4)Fe]_2O$ are 1.775(8) and 1.741(8) Å (av 1.758 Å), and these values can be compared to those found in the analogous, nonbrominated, $[(TPP)Fe]_2O$[11a] of 1.763(1) Å and $[(TPFP)Fe]_2O$[11b] of 1.775(1) Å, or in other μ-oxo iron(III) porphyrins.[12−14] The four nitrogen atoms of each porphyrin unit in $[(TPPBr_4)Fe]_2O$ are not equivalent due to the fact that only two of the four pyrrole rings on each macrocycle are brominated. The two brominated pyrrole rings on each macrocycle of $[(TPPBr_4)Fe]_2O$ have an average Fe−N bond length of 2.107(9) Å, which is significantly longer than the average 2.054(9) Å Fe−N distance for the two nonbrominated pyrrole rings of each macrocycle. However, the average of the four Fe−N distances in the brominated dimer is 2.081 Å, and this value can be compared to an average Fe−N distance of 2.087(5) Å in $[(TPP)Fe]_2O$ and 2.088(11) in $[(TPFP)Fe]_2O$.

The two nonequivalent porphyrin macrocycles are in a quasi-staggered configuration being rotated by an angle of 26° to each other while the nitrogen atoms are symmetrically displaced by 0.02−0.03 Å above and below the mean porphyrin plane. The two iron atoms are displaced by 0.51 Å toward the bridging oxygen atom, and the individual pyrrole rings retain their approximate planarity (maximum deviation = 0.03 Å).

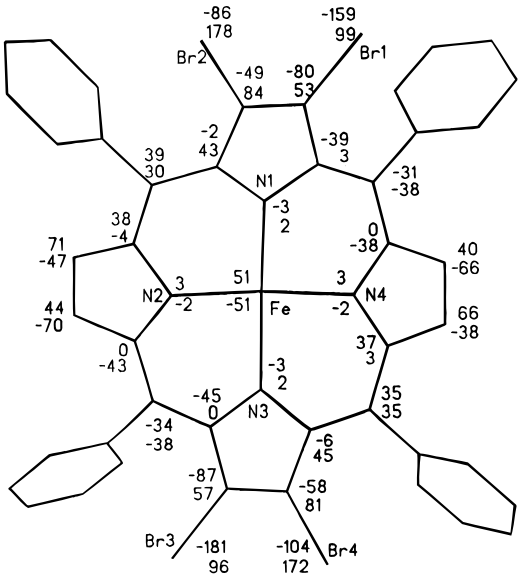

Figure 2. ORTEP diagram illustrating the ruffling of the two porphinato cores of $[(TPPBr_4)Fe]_2O$. The perpendicular displacements of the atoms from the mean plane of the four nitrogen atoms are given in units of 0.01 Å. The upper and lower values refer to the Fe(1) and Fe(2) unit, respectively.

The average distances for N−C_α (1.37(2) Å), C_α−C_β (1.44(2) Å), C_α−$C_{methine}$ (1.40(2) Å), C_β−C_β (1.33(2) Å), $C_{methine}$−C_{phenyl} (1.49(2) Å), and Br−C_β (1.876(15) Å) are comparable to literature data for related porphyrins.[11,15] The S_4 distortion of the porphyrin to a saddle-shape configuration is strongly enhanced as shown in Figure 2. The displacement of the pyrrole β-carbon atoms from the plane of the four nitrogen atoms ranges from 0.38 to 0.87 Å while the displacement of the bromine atoms ranges from 0.86 to 1.81 Å. Moreover, opposite pyrrole rings on the same macrocycle are twisted by about 25° relative to each other so that the porphyrin skeleton ruffling is best described as a twisted saddle-shaped distortion, evidenced by an average displacement of the meso carbon atoms from the porphyrin mean plane by 0.35 Å. The phenyl rings are tilted alternatively up and down and rotated with respect to the mean plane by angles ranging from 49° to 62° to minimize unfavorable contacts with the bromine atoms. It is noteworthy that similar macrocycle rufflings and aryl ring rotations occur in the case of the fully β-halogenated porphyrins,[15] while the tetrahalogenated porphyrins show only a slight distorion from planarity.[6e] Therefore, the severe saddle-shaped deformation found both in monomeric octabromoporphyrins and in the distorted, dimeric tetrabromoporphyrinato μ-oxo iron(III) complex can be likely related to the overall steric and electronic effects of the eight large bromine atoms present in the same chemical unit. Finally, it should be noted that the Soret band of $[(TPPBr_4)Fe]_2O$ (λ_{max} = 419 nm) is red shifted compared to $[(TPP)Fe)]_2O$ (λ_{max} = 410 nm), and this would indicate a saddling of the macrocycle.

The highly halogenated iron μ-oxo dimer is stable in PhCN and *undergoes four one-electron oxidations and four one-electron reductions in a total of seven steps.* Reductions occur at $E_{1/2}$ = −0.78, −1.09, −1.39, and −1.60 V while oxidations

(10) $[(TPPBr_4)Fe]_2O{\cdot}2EtOH{\cdot}H_2O$ crystallizes as red brown platelets unstable in air, leading to the loss of crystallization solvent. Diffraction data were collected at room temperature on a selected crystal fixed in a capillary in the presence of the mother liquor. Crystal data: monoclinic, $P2_1/n$, a = 15.280(2) Å, b = 33.117(7) Å, c = 19.284(2) Å, β = 112.64(1)°, V = 9006(2) Å^3, Z = 4, d(calc) = 1.545 mg/m^3, R = 0.072, R_w = 0.096, s = 1.56, Rigaku AFC5R diffractometer (equipped with a rotating anode), Cu Kα radiation, 11 399 collected reflections, 9578 independent (R_{int} = 0.024), 6695 observed reflections [$F > 4\sigma(F)$]. The data were corrected for absorption (ψ-scan method), Lorentz, and polarization effects. The structure was solved by direct methods and refined by full-matrix least-squares methods (940 variables segmented into three blocks).

(11) (a) Hoffmann, A. B.; Collins, D. M.; Day, V. W.; Fleisher, E. B.; Srivastava, T. S.; Hoard, J. L. *J. Am. Chem. Soc.* **1972**, *94*, 3620. (b) Gold, A.; Jayaraj, K.; Doppelt, R.; Fisher, J.; Weiss, R. *Inorg. Chim. Acta* **1988**, *150*, 177.

(12) Landrum, J. T.; Grimmet, D.; Haller, K. J.; Scheidt, W. R.; Reed, C. *J. Am. Chem. Soc.* **1981**, *103*, 2640.

(13) Collamati, I.; Dessy, G.; Fares, V. *Inorg. Chim. Acta* **1986**, *11*, 149.

(14) Scheidt, W. R.; Lee, Y. J. *Struct. Bonding* **1989**, *64*, 1−70.

(15) (a) Mandon, D.; Oschenbein, P.; Fisher, J.; Weiss, R.; Jayaraj, K.; Austin, R. N.; Gold, A.; White, P. S.; Brigaud, O.; Battioni, P.; Mansuy, D. *Inorg. Chem.* **1992**, *31*, 2044. (b) Ochsenbein, P.; Mandon, D.; Fischer, J.; Weiss, R.; Austin, R.; Jayaraj, K.; Gold, A.; Terner, J.; Bill, E.; Muther, M.; Trautwein, A. X. *Angew. Chem., Int. Ed. Engl.* **1993**, *32* (10), 1437. (c) Birnbaum, E. R.; Hodge, J. A.; Grinstaff, M. W.; Schaefer, W. P.; Henling, L.; Labinger, J. A.; Bercaw, J. E.; Gray, H. B. *Inorg. Chem.* **1995**, *34*, 3625. (d) Grinstaff, M. W.; Hill, M. G.; Birnbaum, E. R.; Schaefer, W. P.; Labinger, J. A.; Gray, H. B. *Inorg. Chem.* 1995, 34, 4896.

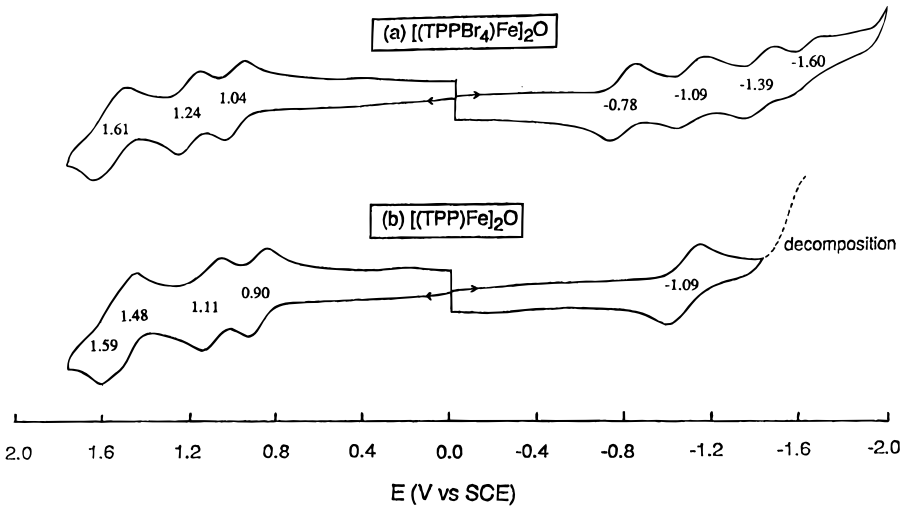

Figure 3. Cyclic voltammograms of (a) $[(TPPBr_4)Fe]_2O$ and (b) $[(TPP)Fe]_2O$, in PhCN, 0.1 M TBAP, at a scan rate of 0.1 V/s.

Table 1. Half-Wave Potentials (V vs SCE) in PhCN, 0.1 M TBAP

	oxidation				reduction			
complex	4th	3rd	2nd	1st	1st	2nd	3rd	4th
$[(TPPBr_4)Fe]_2O$	+1.61[a]	+1.61[a]	+1.24	+1.04	−0.78	−1.09	−1.39	−1.60
$[(TPP)Fe]_2O$	+1.59	+1.48	+1.11	+0.90	−1.09	−1.60		
$(TPPBr_4)FeCl$[b]			+1.56	+1.26	−0.07	−0.86	−1.37	
$(TPP)FeCl$[b]			+1.52	+1.20	−0.29	−1.06	−1.73	

[a] Two overlapping one-electron oxidations. [b] Reference 3b.

are seen at $E_{1/2} = 1.04$, 1.24, and 1.61 V (see Figure 3). The last two oxidations are overlapped in potential, similar to what has been reported for a variety of μ-oxo dimers.[16,17] The same maximum current is measured for the six nonoverlapping processes, each of which has a 60−70 mV separation between E_{pa} and E_{pc}, therefore indicating electrode reactions which involve the addition or abstraction of one electron per dimeric unit.

There is only a single published example of a μ-oxo iron porphyrin dimer which undergoes four reversible one-electron reductions. The investigated compound was $[(TPP(CN)_4)Fe]_2O$, which also contains four electron-withdrawing substituents on each macrocycle. This compound is reduced at −0.07, −0.22, −0.69, and −0.87 V in DMF containing 0.1 M TBAP.[18] However, its electrochemistry was not examined in detail nor was the site of electron transfer elucidated. On the other hand, iron porphycene dimers of the type $[(Pc)Fe]_2O$, where Pc = the dianion of octaethylporphycene (OEPc), etioporphycene (EtioPc), tetrapropylporphycene, (TPrPc) or tetra-*tert*-butylporphycene (TBuPc), also undergo four reductions and four oxidations.[19] For these compounds, the $\Delta E_{1/2}$ between the second and the third reductions (300−400 mV) is much larger than the $\Delta E_{1/2}$ between the first and second (110−190 mV) or third and fourth processes (190−260 mV) for the same compound, and this contrasts with results in the present study where $\Delta E_{1/2}$ between each two subsequent electroreductions ranges from 210 to 310 mV with no obvious trend.

The number of electrons transferred in the first oxidation and first reduction of $[(TPPBr_4)Fe]_2O$ was determined by thin-layer coulometry, while thin-layer spectroelectrochemistry and ESR spectroscopy were used to determine the site of electron transfer in the singly oxidized and singly reduced forms of the dimer. Coulometric data confirm that 0.5 electron per macrocycle (or 1.0 electron per dimer) is added in the first reduction at $E_{1/2} = -0.78$ V and one electron per dimer is abstracted in the first oxidation at $E_{1/2} = +1.04$ V. The neutral μ-oxo dimer is ESR silent due to antiferromagnetic coupling between the two iron(III) central ions, whereas singly oxidized $[[(TPPBr_4)Fe]_2O]^+$ shows a π-cation radical ESR spectrum whose signal is centered at $g = 1.99$ ($\Delta H = 43$ G). The UV−visible spectrum of this monocationic species also supports the assignment of a porphyrin π-cation radical; the intensity of the Soret band is lower than that for the neutral dimer, and the visible bands of the singly oxidized species are all broadened compared to the spectrum of the neutral compound. The doubly oxidized complex is ESR silent.

Table 2. UV−Visible and ESR Spectral Data for Neutral $[(TPPBr_4)Fe]_2O$ and Its Reversibly Oxidized and Reduced Forms in PhCN, 0.1 M TBAP

oxidation state	E_{app} (V)	λ_{max} (nm) $\epsilon \times 10^{-4}$ (M cm^{-1})			g (ΔH, G)
−1	−0.90	418 (15.9)	594 (2.1)	634 (2.2)	1.95 (76)
neutral	0.0	419 (14.5)	598 (2.3)	631 (2.2)	silent
+1	+1.12	419 (14.8)		611 (2.7)	1.99 (43)
+2	+1.40	408 (13.6)		611 (3.5)	silent

Singly reduced $[[(TPPBr_4)Fe]_2O]^-$ is stable on both the spectroelectrochemical and ESR time scales and shows a broad ESR signal centered at $g = 1.95$ ($\Delta H = 76$ G). The UV−vis spectrum of this species is only slightly different from that of the neutral complex (see Table 2), and its ESR spectrum is similar to that of singly reduced $[(TPP)Fe]_2O$ in DMF,[20] a transient species which was assigned to an unstable, ferric−ferrous dimer. A similar metal-centered reduction with formation of a ferric−ferrous dimer, i.e., $[(TPPBr_4)Fe^{III}-O-Fe^{II}(TPPBr_4)]^-$, is proposed in the present study, *but the spectroscopic data of the singly reduced species can also be interpreted in*

(16) Kadish, K. M.; Cheng, J. S.; Cohen, I. A.; Summerville, D. *ACS Symp. Ser.* **1977**, *38*, 65.
(17) (a) Stolzenberg, A. M.; Strauss, S. H.; Holm, R. H. *J. Am. Chem. Soc.* **1981**, *103*, 4763. (b) Chang, D.; Cocolios, P.; Wu, Y. T.; Kadish, K. M. *Inorg. Chem.* **1984**, *23*, 1629.
(18) Kadish, K. M.; Boisselier-Cocolios, B.; Simonet, B.; Chang, D.; Ledon, H.; Cocolios, P. *Inorg. Chem.* **1985**, *24*, 2148.
(19) Kadish, K. M.; Boulas, P.; D'Souza, F.; Aukauloo, M. A.; Guilard, R.; Lausmann, M.; Vogel, E. *Inorg. Chem.* **1994**, *33*, 471.

terms of a delocalization across the orbitals of the two metals and those of the two macrocycles.

Finally, it should be pointed out that the redox potentials of $[(TPPBr_4)Fe]_2O$ are all anodically shifted compared to those of $[(TPP)Fe]_2O$ under the same solution conditions (see Table 1). However, as is also the case with $(TPPBr_x)FeCl$[3] and (TPP)FeCl, the effect of Br substituents on $E_{1/2}$ values is not the same for each electrode reaction[3] and the shift in $E_{1/2}$ with increased bromination is larger in the case of reduction. In fact, the $E_{1/2}$ values for the first reduction of $[(TPPBr_4)Fe]_2O$ (−0.78 V) and $[(TPP)Fe]_2O$ (−1.09 V) vary by +310 mV, a separation which is more than double the difference between the first or second oxidations of the same two compounds where $\Delta E_{1/2}$ is equal to 130 and 140 mV, respectively.

It is now well-known that the introduction of bulky electron-withdrawing substituents mainly lowers the energy of the LUMO, while stabilization of the HOMO will be offset by effects of the macrocycle distortion.[3,6a,21] This also appears to be the case for $[(TPPBr_4)Fe]_2O$ where the full inductive effects of the added Br groups do not influence the oxidation to the same extent as for the reduction, due presumably to the two ruffled macrocycles.

Finally, there is the question of why $[(TPPBr_4)Fe]_2O$ undergoes four reductions compared to only one for $[(TPP)Fe]_2O$ under the same solution conditons. The answer might simply be an increased stability of the electroreduced product due to the presence of electron-withdrawing substituents. However, further studies are now in progress in order to clarify this point.

Acknowledgment. Support from the Robert A. Welch Foundation (KMK, Grant E-680) and the CNR from Italy is gratefully acknowledged. We also thank Mr. G. D'Arcangelo for recording mass spectra, Mr. A. Leoni for his valuable technical support, and Mr. C. Veroli for technical assistance in the X-ray measurements.

Supporting Information Available: Crystal structure determination and refinement, drawings of the dimeric μ-oxo unit with labeling scheme, atomic coordinates, thermal parameters, bonds lengths, and bond angles (19 pages). Ordering information is given on any current masthead page.

IC960040X

(20) Kadish, K. M.; Larson, G.; Lexa, D.; Momenteau, M. *J. Am. Chem. Soc.* **1975**, *97*, 282.

(21) (a) Brigaud, O.; Battioni, P.; Mansuy, D.; Giessner-Prettre, C. *Nouv. J. Chim.* **1992**, *16*, 1031. (b) Takeuchi, T.; Gray, H. B.; Goddard, W. A., III. *J. Am Chem. Soc.* **1994**, *116*, 9730. (c) Bhyrappa, P.; Krishnan, V. *Inorg Chem.* **1991**, *30*, 239.